Slab Design Combining Interlocking Blocks With a Structural Sheet

Mikey Alexander R.*[1], Shai Feldfogel*[1], Netanel Viner[2], and David S. Kammer†[1]

[1]Institute for Building Materials, ETH Zurich, Switzerland

[2]Independent Researcher

November 23, 2023

*Co-first author.

†Corresponding author: dkammer@ethz.ch

Abstract

The construction of structural slabs is one of the more complex, costly, time consuming, and hazardous processes in constructing buildings. This is mainly due to the on-site formwork placement, reinforcement arrangement, and concrete pouring — all required for commonplace slab designs. In theory, industrialization-ready slab designs pose a promising path towards overcoming these challenges. However, designs that can fully deliver on this promise do not yet exist. Hereby, we present a new structural slab design fit for an industrialized construction framework. It is made of interlocking blocks that are adhesively bonded to a structural sheet. We first present the slab design, detail the rationale behind it, and illustrate its inherently quick and accurate construction technique. Then, using numerical simulations, we examine the structural action of the proposed design and how it compares with that of a typical reinforced concrete slab with the same material quantities. We find that the structural performance of the proposed design is competitive with that of a reinforced concrete slab in terms of stiffness, carrying capacity, and ductility. Our results show that the inherently superior constructability of the proposed design is achieved without critical sacrifice of performance, thus underscoring its promising potential as a viable structural design alternative.

1 Introduction

It is on floors where our lives in buildings take place. Occupiable floor space is what we construct them for, after all. Structural slabs — the building elements that support its floors — take up a significant share of total costs, time, and resources consumed in the construction process [1–4]. In certain situations, these might add up to be prohibitively expensive and thus outright prevent project development. This, for example, can prevent the expansion of housing supply, and further exacerbate housing shortages plaguing many countries [5].

Although tried and tested, commonplace slab designs and their associated construction methods still leave room for improvement in terms of efficiency and economy, as evidenced by the common occurrence of construction projects experiencing cost overruns, schedule delays, and excess material waste [6]. In terms of safety, job sites are some of the most hazardous work environments, which is reflected in the industry's relative share of global occupational injuries [7]. The most notable example of such design is the ubiquitous reinforced concrete slab whose construction methods involve numerous labor-intensive and potentially perilous processes, including erection of scaffolding, arrangement of reinforcement steel, and manual pouring of high pressure pumped concrete — all while working at height.

Industrialized Building Systems (IBS) offer many advantages over present-day commonplace methods: time and cost savings, improved quality control, enhanced safety, waste reduction, and more [8, 9]. As such, IBS pose a promising avenue to overcome many of the shortcomings of commonplace methods. Since the design of a building system is closely interrelated with the production of its components and its construction process, creating a design fit for an IBS framework requires an integrated process which has to be planned and coordinated accordingly. In that regard, IBS designs are expected to posses three key traits [8]. First, many of their components are prefabricated offsite, where specialized equipment and organization can be purposefully established. Second, material and component handling onsite is mechanizable. Third, automatized mechanization may be introduced into the construction process in order to further improve productivity and quality and reduce human labor-intensity.

While industrialization is a promising approach to overcoming the drawbacks of commonplace building systems, commercially available structural slab designs incorporating industrialzed components, such as Hollow-core Slabs or Steel Decking Slabs, still rely on in situ reinforced concrete castings [8]. As such, their construction processes still involve all of the aforementioned labor-intensive tasks, which prevents reaping the benefits of industrialization. Therefore, the opportunity to introduce an 'industrialization-ready' innovative structural slab design alternative remains.

Aiming to meet this challenge, we present a novel structural slab design. Its 'plug-and-play' construction process involves assembling a set of interlocking blocks atop a preset structural sheet applied with structural adhesive, which later functions as an integral component of the finalized system. The objective of this study is to demonstrate that our design solution is essentially fit to reap the benefits of industrialization, all while providing adequate structural performance.

Hereafter, in Section 2, we present our design — what it is, and how it can be constructed. In Section 3, we discuss the underlying rationale of our design. In Section 4, we establish the viability of our design as a structural slab for civil applications and validate our design rationale through two case-studies. Lastly, in Section 5, we discuss the results.

2 Design Exposition

Integrative thought, which considers production processes in their entirety — from the conceptual design phase all through the final assembly — is needed to design Industrialized Building Systems (IBS) [8]. To account for this, the presentation of our design addresses both **what** it is — in terms of geometry formed by materials, and **how** it is assembled — in terms of its construction method.

2.1 "The What": Geometry and Materials

Our design consists of two main elements — an assembly of interlocking blocks adhered to a structural sheet (STS). The blocks are of the same geometry, shown in Figure 1a. They are arranged in a repetitive alternating pattern, which when fully assembled, forms a plate-like slab — see Figure 1. Structural adhesive is applied to the interface between the block-formed slab and the STS, resulting in a bonded composite system, as shown in Figure 1c.

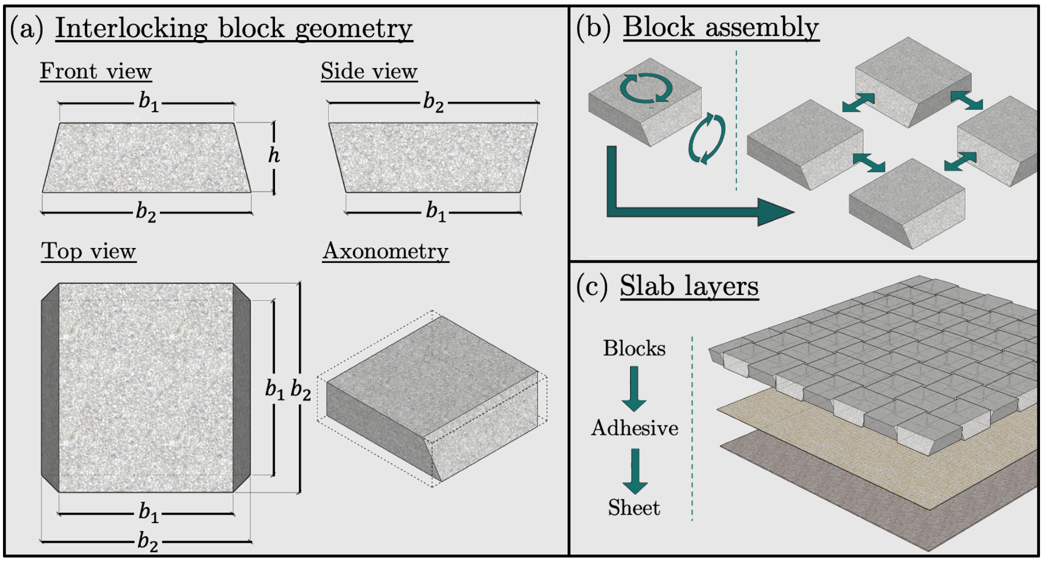

Figure 1: Illustration of our design. (a) Geometric definition of a single block. (b) Fitment of blocks into a plate-like slab. (c) Layers of the complete slab system.

To understand how the resultant structure functions when subject to transverse loads incumbent upon structural slabs, it is simplest to think of its elements in terms of compression and tension, analogous to force couples developing in spanning structures subject to bending moments.

The compressive element is the interlocking block assembly. Its standalone load-bearing static scheme can be thought of as a compression-only truss that is formed within its bulk [10, 11], with the forces transmitted between its members through contact and friction, as depicted in Figure 2. Therefore, a suitable block material must be strong and stiff in compression and have sufficient friction coefficients, but does not require significant tensile capacity. Concrete is suitable, and was chosen for this study, though recent developments in recycled materials point to additional alternatives that pose the potential of greater sustainability [12].

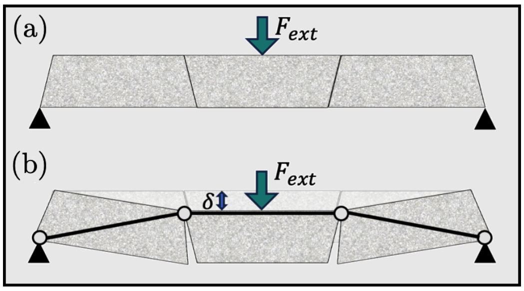

Figure 2: The truss-like static scheme of the interlocking blocked assembly, as formed under transverse loads. (a) Initial state, and (b) deflected state.

The tensile element is the STS. As loading forces increase and displacements get larger, substantial in-plane tensile forces develop in the STS, causing it to function similarly to a membrane. As such, it requires high tensile stiffness, strength, and a high degree of ductility. Potential candidates are steel, cross laminated timber, and to a lesser extent, carbon fiber reinforced sheets. For this study, steel was selected.

The adhesive layer bonds the blocks and the STS into a composite system by transmitting shear and tensile forces between them. To ensure the fullest realization of the slab's potential flexural response, the material of the adhesive must have sufficient shear and tensile stiffness and strength.

As for the connection to the rest of the structural system, the slab is supported on and connected to beams along its edges, as illustrated schematically in Figure 3. Blocks along the edges and at the corners have geometries of symmetrically-cut halves and quarters of the typical blocks, respectively, such that their outer faces along the slab's edge are vertical. Moreover, they have connection details for attachment to the framing supporting the slab. The structural sheet can have machined holes or slots for this purpose. This allows for rivets, preinstalled in the beams as per Figure 3, to bind the assembly, resulting in a simply-supported slab edge.

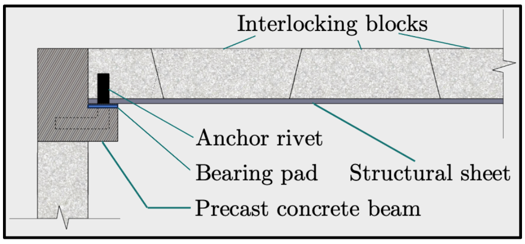

Figure 3: Schematic Beam–Slab connection detail.

2.2 "The How": Construction Method

The fact that our design consists of prefabricated discrete solid elements, makes it suitable for an industrialized construction framework which provides for its inherent advantages such as automation, quality improvement, and faster construction speeds. Joining it to a structural system of beams and columns, ideally prefabricated too, results in a wholly prefabricated structural system. This enables a thoroughly industrialized, and hence advantageous, construction process, as discussed in Section 1.

The construction method we propose consists of four steps — see Figure 4: (1) Erection of telescopic legs. (2) Placement of sheet on top of the telescopic legs, thus creating a flat platform. (3) Application of structural adhesive and simultaneous assembly of the interlocking blocks in sequence. (4) Removal of the telescopic props with the block assembly completed and the adhesive cured, thus completing the process which can then be repeated on the floor above.

The simple nature of this method should prove it easier to mechanize and automate in the future — thereby realizing the potential industrialized construction offers. Additionally, this method offers a significant advantage over commonplace practices which involve in-situ concrete castings: it can be fully operational within 24 hours, the time frame usually required for structural adhesives to sufficiently cure. In comparison, concrete typically requires at least three days of curing time before formwork can be removed and at least seven days before telescopic props can be removed[1], thus taking up operational space on the construction site and costing expensive time in the process.

[1] Per IS-456 (2000) — Plain and Reinforced Concrete — Code of Practice

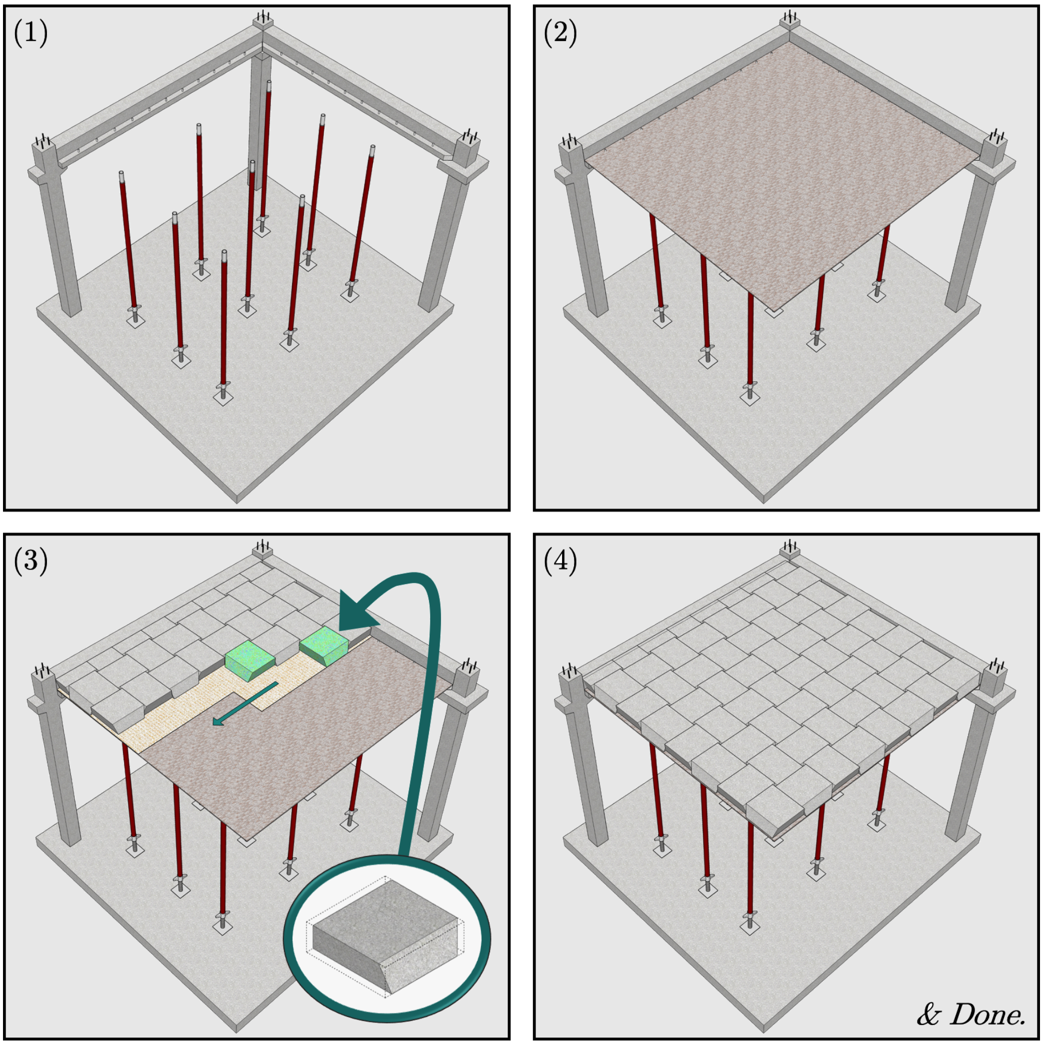

Figure 4: Illustration of the construction process. (1) Erection of telescopic props. (2) Placement of sheet. (3) Application of structural adhesive and simultaneous assembly of the interlocking blocks. (4) With all components in place and adhesive cured — the process is done.

3 Design Rationale

Our structural slab design yields a whole that is greater than the sum of its constituents. In the following discussion, we detail **why** that is so by presenting the reasoning behind our design choices. Our objective is to articulate the necessity of these choices, and to demonstrate their sufficiency as they pertain to our design fulfilling its purpose as a structural slab for civil applications.

Building structural systems are expected to perform in two types of situations during their usable lifespans[2]: serviceability limit states[3] (SLS), which concern the routine demands of everyday use, and ultimate limit states[4] (ULS), which concern edge-case scenarios such as earthquakes and hurricanes that place the safety of the structure and its occupants at risk. The function of a structural system is to provide adequate carrying capacity and occupant comfort in SLS, and to withstand catastrophic failure in a safe and predictable manner in ULS. In structural performance terms, SLS requires sufficient stiffness, and ULS requires strength and ductility. These core concepts will be referred to in the context of the following discussion.

3.1 Starting Point: Interlocking Blocks

Interlocking assemblies are known in the literature as Topologically Interlocking Materials [13–15], or Structures (TIS) [16, 17]. Each block, as part of the assembly, is shaped so that its surfaces mutually align with neighboring blocks. TIS can be constructed quickly and accurately as each block's fit in its designated place is governed by its neighboring blocks. In essence, the

[2]Defined in Eurocode EN-1990 Section 2.3 as "Design Working Life"

[3]See Eurocode EN-1990, Section 3.4: Serviceability Limit States.

[4]See Eurocode EN-1990, Section 3.3: Ultimate Limit States.

core principle is analogous to that of puzzles'.

TIS are non-bonded; they have structural integrity due to contact and friction forces that arise at the interfaces of their interlocking-shaped blocks. Three-dimensional interlocking of TIS blocks enables their assembly into plate-like slabs, which can transmit lateral loads and act as two-way flexural members. To this end, they are resistant to crack propagation, highly energy absorbent, and easily constructible [13, 18].

Owing to these promising traits, TIS slabs have recently been proposed to function as structural slabs in buildings [19, 20]. However, the structural response of standalone TIS slabs exhibits adverse phenomena which practically prohibit their implementation in civil-structural applications.

Foremost are TIS slab mode-of-failure mechanisms which involve block detachment and fall-off, typically near concentrated loads — see Figure 5. Such fall-off mechanisms endanger occupants and raise the risk of progressive collapse of the entire structure [21]. Furthermore, structural global instabilities may arise due to block slippage. Slippage emerges suddenly and causes drops in load-bearing capacity until blocks are rearranged and equilibrium is re-established — see Figure 5a. Occurrences of slippage can introduce adverse dynamic effects, and lead to reduced load capacity and ductility [22, 23]. These phenomena result in difficult-to-predict, non-ductile, and potentially catastrophic structural performance of TIS slabs in edge-case scenarios, thereby not filling ULS requirements.

Next is the low flexural stiffness typical to TIS slabs, which is a direct consequence of the lack of tensile force components [24]. Subject to transverse loads, the blocks compress against each other through progressively decreasing contact regions, thereby undergoing large rotations which cause large gaps to form in the slab — a phenomenon known as 'hinging' [25]. This load-carrying scheme typically results in insufficient stiffness [19], thereby not fulfilling SLS requirements.

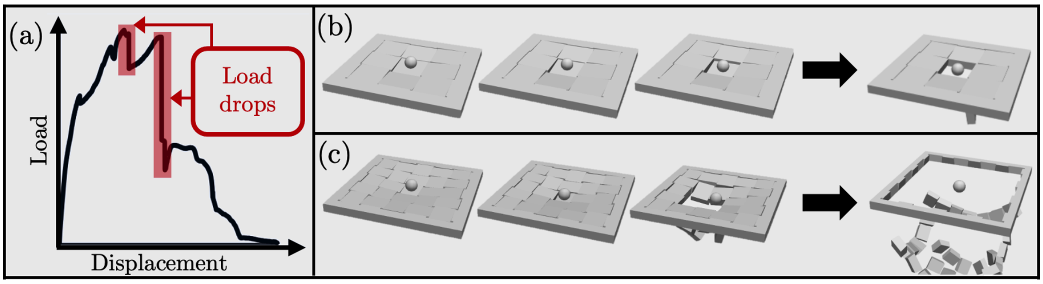

Figure 5: Adverse phenomena of standalone TIS slabs. (a) Typical load-displacement curve of a standalone TIS Slab [23, 26]. (b) Example of a failure mode in which the central loaded block falls off. (c) Example of a failure mode in which the entire block assembly falls off.

3.2 Catastrophe Aversion: Structural Sheet

The fundamental innovation of our proposed design is the introduction of the structural sheet (STS). It serves a dual purpose: first, it acts as a platform and temporary support during construction (see Figure 4); second, and most importantly, it functions as an essential structural component of the finalized slab — specifically, a component that mitigates the structural performance shortcomings of the block assembly (see Section 3.1).

First, the STS averts catastrophic failure modes by preventing blocks from falling off. Second, the STS restrains slippage as it begins to develop, mitigating it and thereby reducing its adverse effects, such as sudden load drops. Third, the STS can significantly increase the overall ductility of the slab system, providing that a ductile material is specified for it. This can manifest in larger work-to-failure energy and higher peak loads reached at larger displacements. Lastly, the presence of the sheet supplies additional redundancy to the slab system, thus reducing risks of catastrophic failure modes such as progressive collapse.

Although the STS can significantly contribute to ULS performance, SLS performance inadequacy remains problematic. As discussed in Section 3.1, the phenomenon of 'hinging' causes the block assembly to lack stiffness as a structural slab. In a non-bonded TIS-STS system, the STS may restrain this phenomenon and contribute some stiffness. Yet, since its structural function is mainly membrane-like, its ability to meaningfully restrain 'hinging' and increase stiffness can only be obtained under large displacements. Thus, the result is that structural stiffness is absent exactly where it is needed most — at small displacements caused by the initial increments of routine loads. Therefore, although most of the structural performance shortcomings of the block assembly can be addressed by the addition of the STS — namely those related to ULS — the issue of SLS stiffness inadequacy remains.

3.3 Performance Enhancement: Structural Adhesive

The addition of the structural adhesive (SA) is aimed at providing a solution to the cardinal issue of inadequate stiffness. By bonding the block assembly — the system's compressive element, to the STS below — the system's tensile element, a flexure-resisting force couple can develop. Thus, by facilitating composite action under the smallest of displacements as the initial increments of transverse loads are applied to the slab, the SA can improve utilization of the components' materials. Critically, this is expected to enable the combined slab system to meet the SLS performance requirements of building codes.

4 Analysis

We conduct two case studies in order to validate that the intended consequences of our design decisions materialize — namely, the expected benefits we described in Section 3. Moreover, we aim to demonstrate that our design can be considered for use in practice. The order of the case studies matches that of our design decisions — each case pertains to each incremental addition we made, thus isolating their marginal effects and showcasing their respective contributions. The first focuses on the addition of the STS to the block assembly. The second focuses on the addition of the SA to the system, and how it confers the design its viability for civil applications.

The specimens we examine are subject to typical load types, and with boundary conditions — accounting for supports — uniformly defined along the slab perimeters. In both cases, we consider realistically sized slabs spanning 5 by 5 meters, made of concrete TIS slabs whose individual block dimensions are parametrically defined in Figure 1: $b_1 = 777$ $[mm]$, $b_2 = 833$ $[mm]$, $h = 318$ $[mm]$. The steel STS, where applicable, is 6 $[mm]$ thick. This choice allows for a *ceteris paribus* comparison of our design with reinforced concrete slab: utilizing equivalent material quantities with the same boundary and loading conditions. With all resultant specimens and applied loads doubly symmetric, we analyse one quarter of their structures and accordingly apply boundary conditions at the symmetry edges, see Figure 6

We conduct the case studies using Finite Element Method (FEM) simulations, and that is for two reasons. First, FEM simulations are a standard approach to examine early-stage design phases, particularly as a precursor to physical prototype testing. Second, they are uniquely suitable to capture and illustrate the intricate and highly non-linear structural-mechanical features that characterize our design: the contact and friction forces between the discrete blocks and between the block assembly and the sheet (contact non-linearity), the crushing of the blocks and the yielding of the sheet that are expected to govern the failure process (material non-linearity), and the large displacements that are expected to occur at high load levels (geometric non-linearity). For additional information regarding the computational methodology of our analyses, see Appendix A.

4.1 Case Study A: Benefits Provided by the Sheet

The purpose of the first case study is to demonstrate how the addition of the STS to the interlocking block assembly provides significant improvements to the structural performance of the combined structure in ULS scenarios, specifically by: (1) the elimination of catastrophic modes of failure plaguing TIS slabs, (2) restraint of load-drops, and (3) increased global ductility.

We compare a standalone TIS slab (specimen A1) with an identical TIS slab placed on an STS (specimen A2), and with the boundary conditions shown in Figure 6. Both specimens are centrally-loaded with an external displacement-controlled rigid body, simulating the action of a concentrated load. This type of loading was chosen because it most suitable to exemplify the problematic fall-off failure modes of TIS slabs, and their solution via the STS addition.

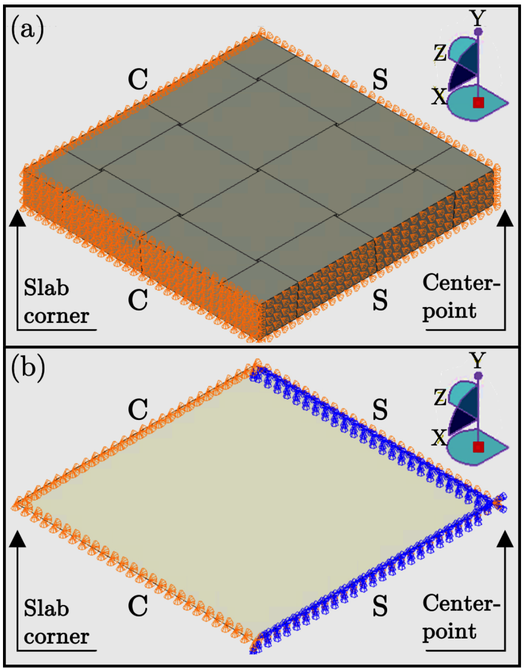

Figure 6: Computational definition of boundary conditions. (a) TIS slab: Clamped faces **C** have all translation degrees of freedom (DOF) constrained, resulting in a fixed clamped slab edge. Symmetry faces **S** have perpendicular translation DOF constrained, resulting in a rolling clamped slab edge. (b) STS: Edges **C** have all DOF constrained, resulting in a pinned plate edge. Symmetry edges **S** have perpendicular translation and rotation DOF constrained, resulting in a rolling clamped plate edge.

Comparing the load-deflection curves of specimens A1 and A2 — shown in Figure 7 — we find that specimen A1 reached a peak load of 242.9 $[kN]$ at a deflection of 81.1 $[mm]$. Specimen A2 reached a peak load of 373.6 $[kN]$ at a deflection of 272.3 $[mm]$. Thus, the addition of the STS results in a peak load that is 53.8% higher, and is reached at a deflection that is 3.37 times larger — evidencing that the increase in strength is also provided with significantly enhanced ductility. The increasing divergence in carried loads (see the outlines of area (W)) shows that the contribution of the STS to the structural response grows more significant with larger load- and deflection-levels. Work-to-failure energy of the specimens totals 36.5 $[kN \times m]$ for A1 and 69.6 $[kN \times m]$ for A2 — an increase of 90.7%, which serves as additional evidence of the improvement in ductility. Arrows (1–3) mark occurrences of load-drops in the response of A1 — after two initial occurrences in (1) and (2), occurrence (3) begins a slump that continues until failure. In contrast, observe arrows (I–III) which mark A2's curve. After two initial bouts of load-drops, albeit at higher loads and deflections than A1, an essential inflection happens at (III) — that is where the contribution of the STS shows its merit, as it prevents a further slump in strength and enables the structure to reach the higher peak load and larger deflection it does. Examining the curves in the range of small displacements, we observe that they track almost identically; thus, we infer that flexural stiffness — in the range it matters — is not improved by the addition of the STS.

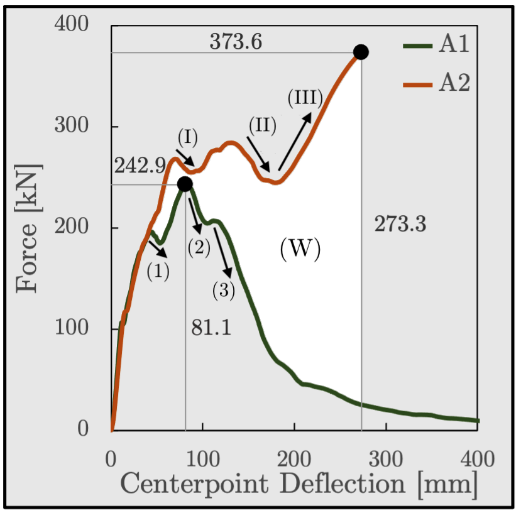

Figure 7: Load-deflection curves of specimens A1 and A2. Highlighted integral area between the curves, marked by (W) represents the cumulative difference in energy absorption up to the point A2 reaches its peak load. Peak loads and corresponding displacements also marked by black dots, with their measured values noted on outbound adjacent lines. Arrow series (1–3) and (I–III) accentuate the differences in the developments of the structural responses of A1 and A2, respectively.

Next, we consider the snapshots of the modes-of-failure of the specimens in Figure 8. The catastrophic mode-of-failure of specimen A1, shown in Figure 8a, has its central block detach and fall off. This structural behavior breaches the *sine qua non* requirement of occupant safety in ULS, as discussed in Section 3.1. As for specimen A2, its mode-of-failure has the STS catching the block and preventing it from falling off, see Figure 8b.

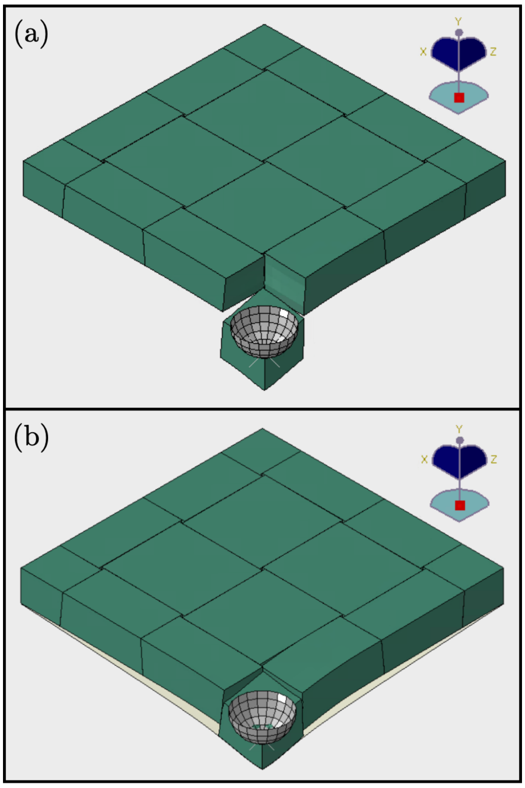

Figure 8: Modes of failure in case study A: (a) Specimen A1 — central block detaches and falls off, and (b) Specimen A2 — STS catches the central block.

This case study provides four main insights regarding the addition of the STS: (1) Catastrophic failure, involving structural components detaching and falling off, has been mitigated; (2) The phenomenon of load drops has been restrained at its critical inflection point; (3) Global ductility is vastly increased, and in multiple aspects: total work-to-failure energy, magnitude of peak load, and the corresponding deflection it is reached at. Although it may be trivial to expect that the addition of a load-bearing component to an existing structure can improve its performance, considering that the thickness of the STS is only 2% of that of the TIS slab, the resultant improvement is significant — thus showcasing the impactful marginal effects of the STS addition; (4) The addition of the STS, by itself, does not solve the problem of flexural stiffness insufficiency of the standalone TIS slab.

4.2 Case Study B: Addition of Adhesive

The second case study serves a dual-purpose. Foremost, it serves to validate the assumptions we have made in Section 3.3 regarding the contributions of the SA, namely — its necessity in achieving sufficient flexural stiffness. Second, to show that our design is competitive with a monolithic reinforced concrete slab (RC) — an exemplar of present-day commonplace structural slabs in terms of structural performance.

First, to isolate the marginal contributions of the SA, we compare a specimen of a concrete TIS slab placed atop a steel STS (specimen B1) to an identical specimen which has the SA applied to its TIS-STS interface (specimen B2), both subjected to an incrementally increasing uniform distributed load and simply-supported at their perimeter edges, see Figure 9. Specimen B2 is representative of our complete design.

Then, to this comparison we add an RC slab that is 324 [mm] thick, reinforced with 20 [mm] steel bars placed every 105 [mm] at its bottom face, and has a concrete cover thickness of 20 [mm] — providing for a *ceteris paribus* comparison: all examined specimens utilizing equivalent quantities of concrete and steel, having equivalent total thicknesses and span lengths, supported by identical boundary conditions, and subject to the same loading conditions.

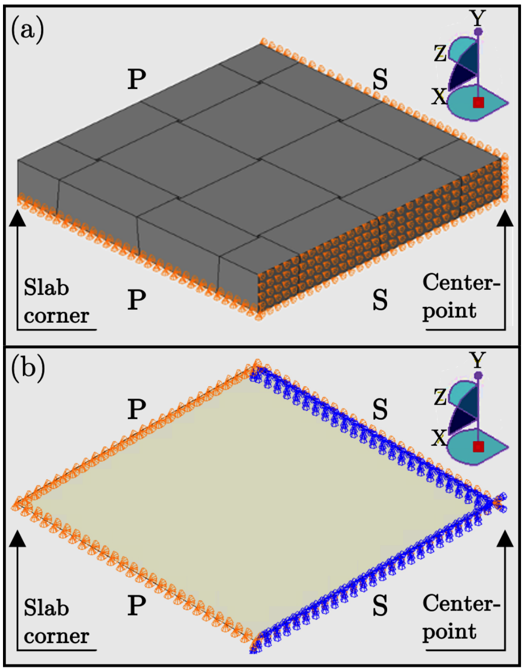

Figure 9: Definition of boundary conditions. (a) TIS slab: edges **P** have all translation DOF constrained, but rotation DOF unconstrained, resulting in a simply-supported slab edge. Symmetry faces **S** have perpendicular translation DOF constrained, resulting in a rolling clamped slab edge. The same modelling technique was applied to the RC slab specimen. (b) STS: Edges **C** have all DOF constrained, resulting in a simply-supported plate edge. Symmetry edges **S** have perpendicular translation and rotation DOF constrained, resulting in a rolling clamped plate edge.

4.2.1 Marginal Benefits Provided by the Adhesive

Examining the load-deflection curves of specimens B1 and B2 shown in Figure 10, we observe the increased flexural stiffness provided by the addition of the SA. Focusing on the initial part of the curve, which is shown in the zoomed-in plot, we can directly compare the stiffness of the specimens. Building codes typically specify a deflection of around Span/250 as a serviceability limit criterion[5]. In our case, this amounts to a deflection of 20 [mm], which in specimen B1 was caused by a load of 0.081 [N/mm^2], and in B2 by a load of 0.263 [N/mm^2] — a significant increase by a factor of 3.23. Specimen B1 would overstep SLS demands simply due to its own self-weight of 0.081 [N/mm^2][6] that leaves no room for any additional load, ruling it unacceptable for civil-structural applications — validating concerns of insufficient stiffness raised in Section 3.1. In contrast, specimen B2 leaves almost 0.182 [N/mm^2] for additional dead- and live-loads.

[5]See Eurocode EN 1992-1-1:2004 Section 7.4.1(4). Though we note that it refers to long-term deflections, which take into account non-linear effects such as concrete creep and shrinkage, effects not accounted for in our analysis.

[6]Per Eurocode EN 1991-1-1, Tables A.1 and A.4: concrete and steel self-weights of 24 [kN/m^3] and 78 [kN/m^3], respectively.

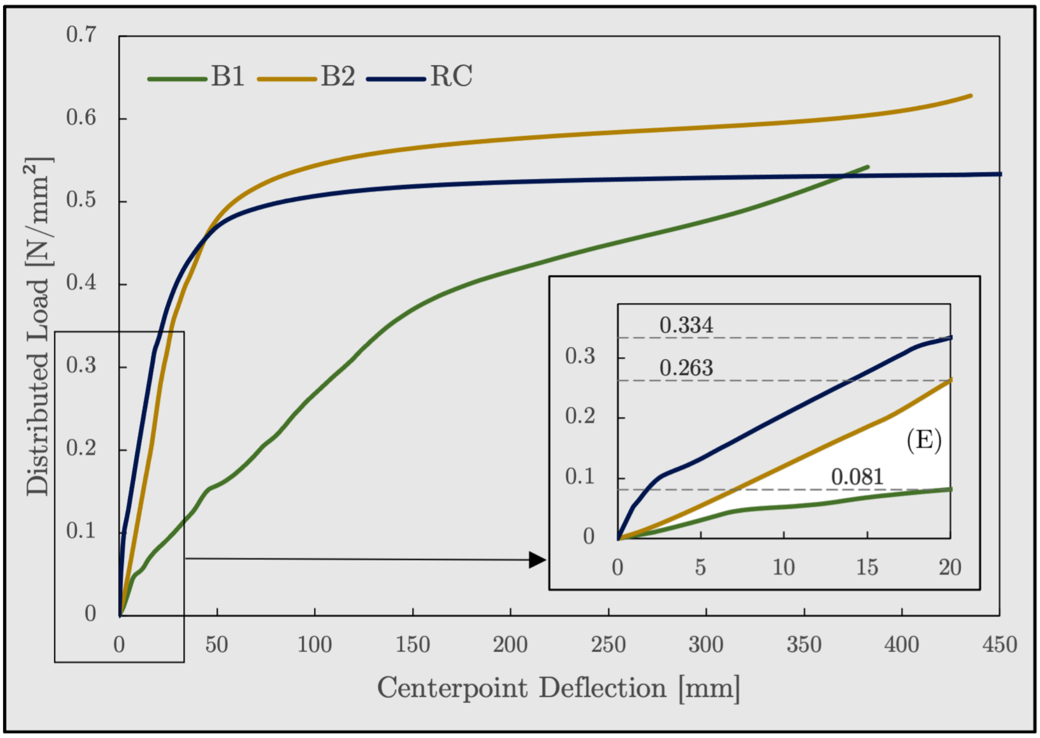

Figure 10: Load-deflection curves of specimens B1, B2 and RC. The zoomed-in area gives a better perspective on initial stiffness, with the expected performance of our design in the range bound by the curves of specimens B1 and B2, marked by the highlighted area (E).

We sampled stresses in the structural components subject to loads of 0.1, 0.2, 0.3, and 0.4 $[N/mm^2]$ to illustrate the differences in evolution of the structural response due to the addition of the SA, shown in Figure 11. A close examination of the results reveals two interesting insights.

First, observing Figures 11b and 11d, we find that in specimen B1, at a load of 0.1 $[N/mm^2]$ the STS is barely utilized, evidenced by uniformly low tensile stress throughout. Yet, as the load increases, stresses in the STS rapidly increase — initially where the corner of the central block pushes against it, and then spreading outwards. This differs from specimen B2, where at a load of 0.1 $[N/mm^2]$, the STS already shows stresses arising where the block interface lines are. Increased loading spreads higher stresses from these interface lines outwards, indicating that the STS is directly restraining the 'Hinging' effect of the TIS slab mentioned in Section 3.1. This comparison demonstrates how the addition of the SA transforms the nature of the structural response of the STS from membrane-like to reinforcement-like, and thus makes for a stiffer slab.

Second, we observe that the composite action enabled by the SA results in lower peak stresses and more uniform stress distribution, see Figures 11b and 11d. This is evident when observing the STS of specimens B1 and B2 at a load of 0.4 $[N/mm^2]$ — while the former is undergoing widespread yielding, the latter barely reaches 50% of its yield stress in almost all of its area. Moreover, we observe that the uneven stress distributions in both the blocks and the STS of specimen B1 at that same load of 0.4 $[N/mm^2]$ differ from the almost-uniform distributions of B2. The same phenomenon affects the block assemblies of the specimens in the same manner. Thus, we infer that the SA facilitates more efficient material utilization.

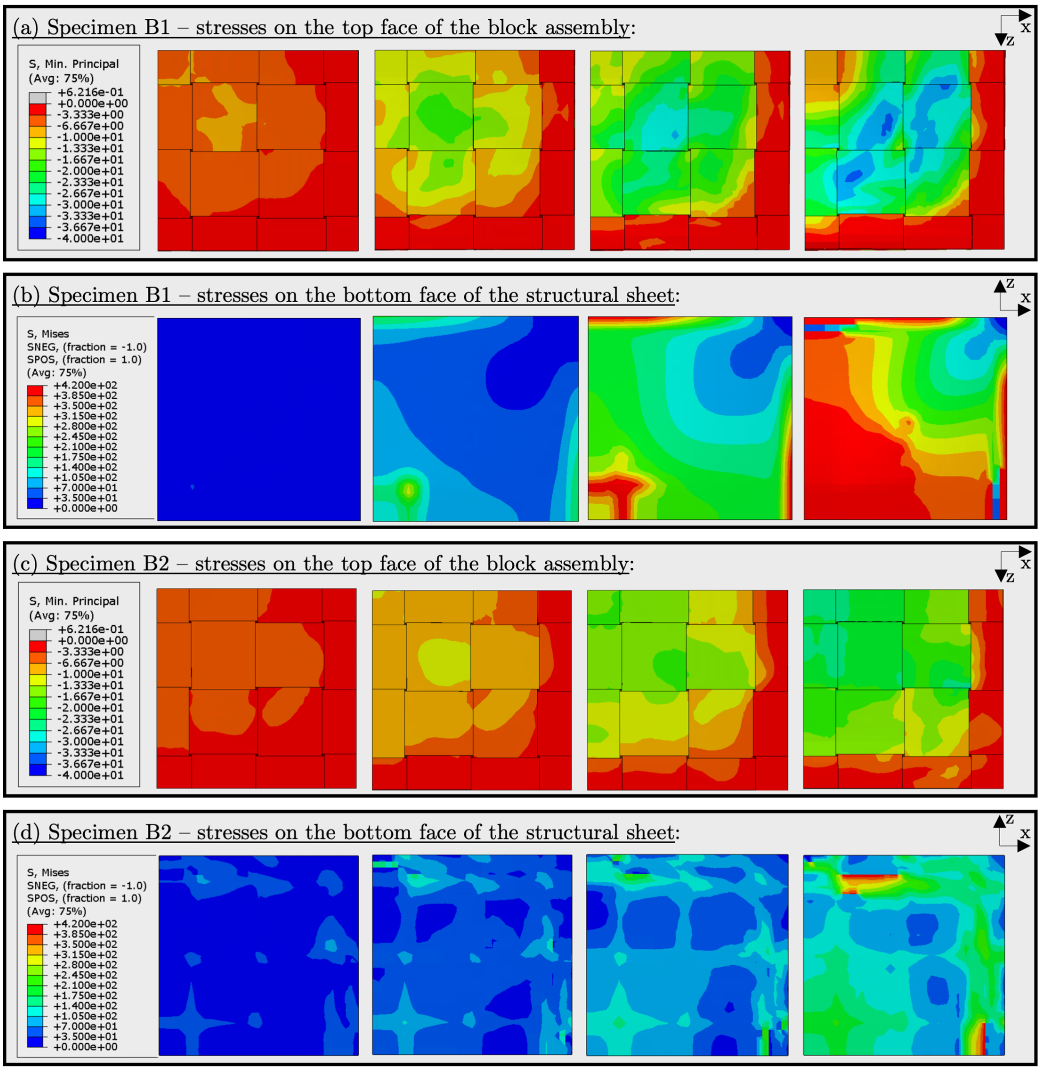

Figure 11: Stresses in structural components subject to loads of 0.1, 0.2, 0.3, and 0.4 $[N/mm^2]$, shown left-to-right, respectively.

4.2.2 Comparison with Reinforced Concrete Slab

The overall structural response of our design — as represented by specimen B2, and how it compares with that of the RC slab, is best understood when examining the load-deflection curves of the specimens in Figure 10. Given how closely both curves track, with that of B2 even achieving higher loads at larger displacements, we find that specimen B2 performs competitively against the RC slab.

Next, we analyse SLS load carrying capacity of the specimen. At the SLS-specified deflection of 20 $[mm]$, the RC slab specimen was subject to a load of 0.334 $[N/mm^2]$, which leaves 0.253 $[N/mm^2]$ for additional dead- and live-loads — 0.071 $[N/mm^2]$ more than B2's 0.182 $[N/mm^2]$. Considering that live-loads in residential and commercial uses typically vary at a range of 0.015–0.050 $[N/mm^2]$[7], with additional dead-loads of 0.010–0.025 $[N/mm^2]$ due to partitions, flooring, and other permanent fixtures, both specimens fulfill SLS requirements.

We note that the actual performance of our design, employing realistic SA with non-ideal structural properties, is expected to fall in the highlighted range (E) in Figure 10 — between the curves of B1, which is completely non-bonded, and of B2, which is fully-bonded. We expect actual physical response to track closer to B2, particularly at the beginning of the curve, and transition to that of B1 at very large displacements, where debonding can occur as a result of SA failure.

In conclusion: the structural bonding provided by the SA has been proven beneficial, as evidenced by increased global stiffness which is increased by a factor of 3.23 over the non-bonded alternative, and has placed it within close range of that of the RC slab — with both deemed adequate by the SLS deflection criterion. Looking beyond initial stiffness required for SLS, the load-deflection curve of B2 exhibits that global ductility is not only preserved with the addition of the SA, but rather, greatly enhanced — resulting in performance quite similar to that of the RC slab. These results show that the significant advantages of our design in aspects of constructability, economy

[7]Per Eurocode EN 1991-1-1, Tables 6.1 and 6.2.

and safety do not come at the expense of structural performance.

5 Conclusion

A novel structural slab design has been presented. This design, inherently fit for an industrialized construction framework, is aimed at overcoming the practical, economical, and safety issues associated with commonplace slab designs. By ridding of processes at the root of these aforementioned issues, such as reinforcement arrangement and concrete pouring, a simple and quick construction method is provided. After outlying the details of the design and explaining the rationale behind it, we have examined its structural action fundamentals in numerical case studies in which we have demonstrated its adequacy in its purpose as a civil-structural slab, as it provides performance competitive with that of the quintessential reinforced concrete slab. These results underscore the promising potential of the proposed design as a viable structural design alternative and its merit of consideration as such.

6 CRediT authorship contribution statement

Mikey Alexander R.: Conceptualization, Methodology, Formal Analysis, Writing — Original Draft, Visualization. **Shai Feldfogel:** Methodology, Formal Analysis, Writing — Original Draft, Supervision. **Netanel Viner:** Formal Analysis, Investigation, Writing — Review & Editing. **David S. Kammer:** Writing — Review & Editing, Supervision.

7 Acknowledgements

Much gratitude is dedicated to Artyum Iounousov — an architect, a designer, and most importantly: a good friend — for his contributions to Figures 1–4.

References

1. Sahab, M. G., Ashour, A. F. & Toropov, V. V. Cost optimisation of reinforced concrete flat slab buildings. *Engineering Structures* **27,** 313–322 (Feb. 1, 2005).
2. Singh, S. Cost Model for Reinforced Concrete Beam and Slab Structures in Buildings. *Journal of Construction Engineering and Management* **116.** Publisher: American Society of Civil Engineers, 54–67 (Mar. 1, 1990).
3. Wang, W.-C., Weng, S.-W., Wang, S.-H. & Chen, C.-Y. Integrating building information models with construction process simulations for project scheduling support. *Automation in Construction* **37,** 68–80 (Jan. 1, 2014).
4. Proverbs, D. G., Holt, G. D. & Olomolaiye, P. O. Factors impacting construction project duration: a comparison between France, Germany and the u.k. *Building and Environment* **34,** 197–204 (Mar. 1, 1998).
5. Corinth, K. & Dante, H. *The Understated 'Housing Shortage' in the United States* Rochester, NY, Aug. 2, 2022.
6. Baloi, D. & Price, A. D. F. Modelling global risk factors affecting construction cost performance. *International Journal of Project Management* **21,** 261–269 (May 1, 2003).

7. Lingard, H. Occupational health and safety in the construction industry. *Construction Management and Economics* **31,** 505–514 (June 1, 2013).
8. Warszawski, A. *Industrialized and Automated Building Systems: A Managerial Approach* 2nd ed. 484 pp. (Routledge, London, Dec. 20, 2019).
9. Li, Z., Shen, G. Q. & Xue, X. Critical review of the research on the management of prefabricated construction. *Habitat International* **43,** 240–249 (July 1, 2014).
10. Khandelwal, S., Siegmund, T., Cipra, R. J. & Bolton, J. S. Transverse loading of cellular topologically interlocked materials. *International Journal of Solids and Structures* **49,** 2394–2403 (Sept. 15, 2012).
11. Khandelwal, S., Siegmund, T., Cipra, R. J. & Bolton, J. S. Scaling of the Elastic Behavior of Two-Dimensional Topologically Interlocked Materials Under Transverse Loading. *Journal of Applied Mechanics* **81** (Sept. 19, 2013).
12. Chen, W. *et al.* Adopting recycled aggregates as sustainable construction materials: A review of the scientific literature. *Construction and Building Materials* **218,** 483–496 (Sept. 10, 2019).
13. Dyskin, A. V., Estrin, Y., Kanel-Belov, A. J. & Pasternak, E. Topological interlocking of platonic solids: A way to new materials and structures. *Philosophical Magazine Letters* **83,** 197–203 (Jan. 1, 2003).
14. Williams, A. & Siegmund, T. Mechanics of topologically interlocked material systems under point load: Archimedean and Laves tiling. *International Journal of Mechanical Sciences* **190,** 106016 (Jan. 2021).
15. Zakeri, M., Majidi, M., Haghighi-Yazdi, M. & Safarabadi, M. Numerical analysis of linear and nonlinear buckling instability of plates made of

topologically interlocked materials. *Mechanics Based Design of Structures and Machines* **51,** 3260–3272 (June 3, 2023).

16. Koureas, I., Pundir, M., Feldfogel, S. & Kammer, D. S. On the failure of beam-like topologically interlocked structures. *International Journal of Solids and Structures* **259,** 112029 (Dec. 25, 2022).

17. Feldfogel, S., Karapiperis, K., Andrade, J. & Kammer, D. S. Failure of topologically interlocked structures - a Level-Set-DEM approach. *European Journal of Mechanics - A/Solids,* 105156 (Oct. 10, 2023).

18. Dyskin, A., Estrin, Y., Pasternak, E., Khor, H. & Kanel-Belov, A. Fracture Resistant Structures Based on Topological Interlocking with Non-planar Contacts. *Advanced Engineering Materials* **5,** 116–119 (2003).

19. Weizmann, M., Amir, O. & Grobman, Y. J. Topological interlocking in buildings: A case for the design and construction of floors. *Automation in Construction. Computational and generative design for digital fabrication: Computer-Aided Architectural Design Research in Asia (CAADRIA)* **72,** 18–25 (Dec. 1, 2016).

20. Piekarski, M. Floor Slabs Made from Topologically Interlocking Prefabs of Small Size. *Buildings* **10.** Number: 4 Publisher: Multidisciplinary Digital Publishing Institute, 76 (Apr. 2020).

21. Starossek, U. Typology of progressive collapse. *Engineering Structures* **29,** 2302–2307 (Sept. 1, 2007).

22. Djumas, L., Simon, G. P., Estrin, Y. & Molotnikov, A. Deformation mechanics of non-planar topologically interlocked assemblies with structural hierarchy and varying geometry. *Scientific Reports* **7.** Number: 1 Publisher: Nature Publishing Group, 11844 (Sept. 19, 2017).

23. Feldfogel, S., Karapiperis, K., Andrade, J. & Kammer, D. S. Scaling, saturation, and upper bounds in the failure of topologically interlocked structures. *International Journal of Solids and Structures* **269,** 112228 (May 1, 2023).

24. Khor, H. C., Dyskin, A. V., Pasternak, E., Estrin, Y. & Kanel-Belov, A. J. in *Structural Integrity and Fracture* 449–456 (Swets & Zeitlinger, Lisse, 2002).

25. Laudage, S., Guenther, E. & Siegmund, T. Design and analysis of a lightweight beam-type topologically interlocked material system. *Structures* **51,** 1402–1413 (May 1, 2023).

26. Mirkhalaf, M., Dastjerdi, A. K. & Barthelat, F. Overcoming the brittleness of glass through bio-inspiration and micro-architecture. *Nature Communications* **5.** Number: 1 Publisher: Nature Publishing Group, 3166 (Jan. 28, 2014).

27. Qingfu, L., Wei, G. & Yihang, K. Parameter calculation and verification of concrete plastic damage model of ABAQUS. *IOP Conference Series: Materials Science and Engineering* **794.** Publisher: IOP Publishing, 012036 (Mar. 2020).

28. Rabbat, B. G. & Russell, H. G. Friction Coefficient of Steel on Concrete or Grout. *Journal of Structural Engineering* **111.** Publisher: American Society of Civil Engineers, 505–515 (Mar. 1, 1985).

A Appendix: Computational Methodology

FEM simulations in this study were done using Abaqus version 2022.HF5, employing the standard static non-linear solver. The models account for geometric, material, and contact non-linearity. A concrete damage plasticity was used for the constitutive modeling of the concrete [27] and a bi-linear elastic-plastic law was used for the steel. The constitutive laws are depicted in Figure 12. The General Contact algorithm was used to enforce the block-block and block-sheet contact using the Hard contact functionality, with isotropic Coulomb friction used for the tangential interactions. The concrete-concrete and concrete-steel friction coefficients were both taken as 0.5 [28]. In case B2, the bonding between the blocks and the sheet was modeled using Tie constraints. To avoid over-constraint of nodes, only the central area of each block was tied to the sheet, see Figure 13. For the monolithic reinforced concrete slab, the Embedded Region functionality was used to model perfect bonding between the concrete and the reinforcement grid, which were modeled with 3D truss elements. C3D8R (an 8-node linear brick with reduced integration and hourglass control) solid elements were used to discretize the blocks. S4R (a 4-node doubly curved thin or thick shell with reduced integration, hourglass control, and finite membrane strains) shell elements were used to discretize the sheet. To ensure a matching mesh between the blocks and the sheet (an important feature for affecting Tie Constraints), a uniform element size of 86 mm was used. The concentrated load indenter in cases A1 and A2 was modeled as a rigid analytical surface.

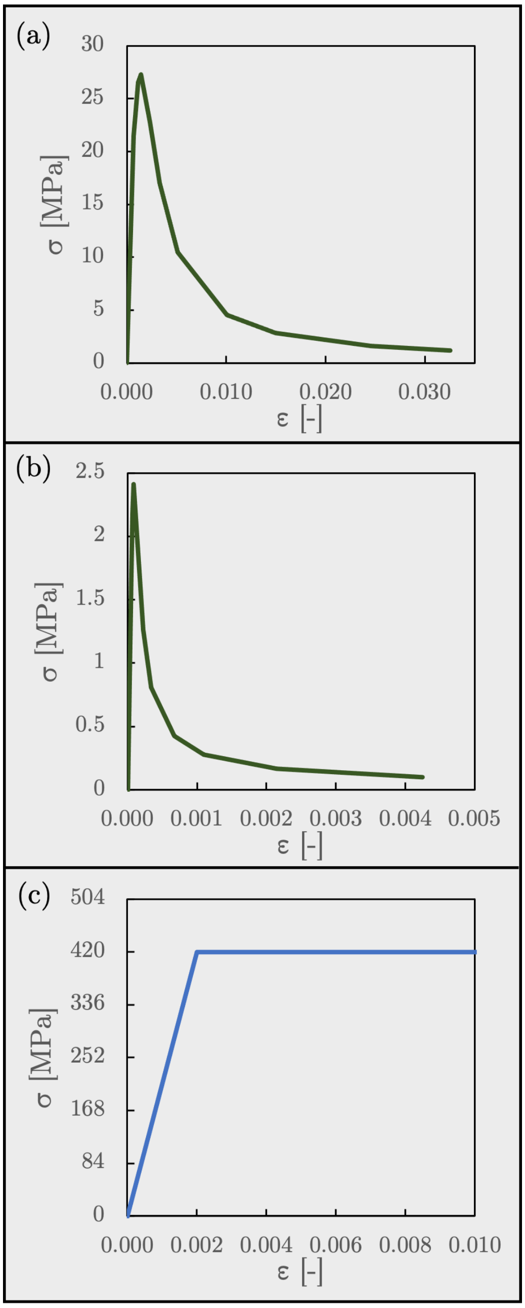

Figure 12: Material constitutive laws. (a) Concrete: progressive damage plasticity compression model. (b) Concrete: progressive damage plasticity tension model. (c) Steel: bi-linear elastic-plastic, identical in tension and in compression.

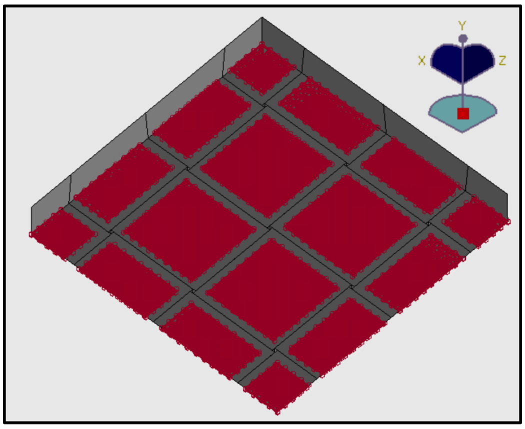

Figure 13: Definition of tie constraints in specimen B2 — marked by the areas in colored in red.